Conference paper

Anton L. Maximov*, Khusain M. Kadiev, Leonid A. Zekel, Agadjan M. Gyul'maliev and Malkan Kh. Kadieva

Particular kinetic patterns of heavy oil feedstock hydroconversion in the presence of dispersed nanosize MoS_2

https://doi.org/10.1515/pac-2020-0204

Abstract: A kinetic model of the heavy oil feedstock hydroconversion performed in continuous flow reactor in the presence of in-situ synthesized dispersed nanosize catalyst Molybdenum disulfide (MoS_2) has been proposed. The kinetic parameters of heavy oil feedstock with different properties have been determined for the two process versions: with coke formation and without appreciable coke formation. It has been stated that hydroconversion in the presence of in-situ synthesized dispersed MoS_2 (C(Mo) = 0.05% wt. (per feed)) corresponds to a first-order reaction for all studied feedstock samples. The rate and activation energy constants have been determined. It has been shown that the conditions of polycondensation products (coke) formation result in increasing process rate and decreasing activation energy.

Keywords: activation energy; dispersed catalyst; heavy oil feedstock; hydroconversion; kinetic model; Mendeleev-21; molybdenum disulfide; rate constant.

Introduction

The observed tendency of heavier oil production displays the problem of heavy feedstock (residues of oil, bitumen and heavy feed distillation) processing. The methods based on traditional solid support stabilized hydrocracking catalysts for such feedstock have been proved to be inefficient. Catalysts quickly lose activity because of deposited polymerization products from thermal degradation of resins and asphaltenes – coke, vanadium and nickel compounds [1, 2]. The use of ultrafine and nanosize dispersed catalysts, which are hydrocarbon-stabilized unsupported suspensions of particles of molybdenum, nickel, cobalt, iron sulfides uniformly distributed in the feed volume, has made significant progress in developing the heavy oil feedstock (HOF) processing technology. However, despite numerous publications confirming the high dispersed catalysts efficiency for hydroconversion of various HOF, the kinetics of the process in flow reaction systems has been less studied.

Several publications address the kinetics of HOF hydroconversion in the presence of ultrafine and nanosize dispersed catalysts. In [3, 4], the authors studied the hydroconversion of Belayim oil residue after vacuum distillation in the presence of a suspension of nanosized MoS_2 particles synthesized from molybdenum naphthenate. The experiments were performed in an autoclave at 410–450 °C. The initial hydrogen pressure was 9 MPa. The authors concluded that the dispersed catalyst had little effect on the distillate product yield, but stabilized radical fragments of resin and asphaltene molecules preventing coke formation. The process corresponds to a first-order reaction.

Article note: A collection of invited papers based on presentations at 21st Mendeleev Congress on General and Applied Chemistry (Mendeleev-21), held in Saint Petersburg, Russian Federation, 9–13 September 2019.

***Corresponding author: Anton L. Maximov**, A.V. Topchiev Institute of Petrochemical Synthesis, Russian Academy of Sciences, Moscow, Russia, e-mail: max@ips.ac.ru

Khusain M. Kadiev, Leonid A. Zekel, Agadjan M. Gyul'maliev and Malkan Kh. Kadieva: A.V. Topchiev Institute of Petrochemical Synthesis Russian Acadmy of Sciences, Moscow, Russia, e mkadieva@ips.ac.ru (M.K. Kadieva)

$$\text{Feed} \rightarrow \text{Reaction product} \quad (1)$$

The activation energy for the hydrocracking process was 147 kJ/mol.

It should be noted that the results of stationary autoclave experiments do not reflect the nature of the reactions in flow reaction systems, since the hydrogen pressure decreases almost three times during the experiment [4].

In Ref. [5], the kinetic parameters of heavy feedstock hydroconversion in the presence of a dispersed MoS_2 suspension synthesized in situ in the feed from the reverse emulsion of an ammonium paramolybdate aqueous solution are given. The experiments were carried out in a flow reactor of an upward flow unit at a temperature of 440–460 °C, a hydrogen pressure of 7.0 MPa and a feed space velocity of 1–3 h^{-1}. The authors found that the 500 °C+ distillation residue conversion to reaction products corresponded to a first-order reaction. The activation energy was 216.8 kJ/mol. The SARA hydroconversion rate increases for asphaltenes, resins, aliphatic hydrocarbons and aromatic hydrocarbons, and the activation energy increases for paraffin–naphthene, aromatic hydrocarbons, resins, asphaltenes. The results obtained are consistent with the SARA conversion principles stated in [6].

The studies of the kinetic characteristics for HOF hydroconversion allow to evaluate the influence of the reaction time on the conditional components yield at the established parameters (temperature, pressure, hydrogen supply, composition, and amount of the catalyst), and can be used to predict data for the process calculation.

Methods and experimental part

Kinetic study

To describe the kinetics of HOF hydroconversion processes in the presence of ultrafine and nanosize dispersed catalysts, various models can be used with different composition, properties, and amount of components. Thus, to describe the hydrocracking kinetics of petroleum distillate fractions as components of the system, phases (gas, liquid product, and coke), technical fractions (vacuum gas oil, diesel, and gasoline fractions), group composition elements, narrow distillate fractions with different boiling point were used in addition to feedstock [7].

As the main purpose of HOF hydroconversion is to obtain distillate fractions, two kinetic models are considered in our study. The first one is the conversion of residual 520 °C+ HOF fractions to products (including gas and the wide distillate initial boiling point (IBP)-520 °C fraction) described by the equation:

$$520^{\circ}\text{C} + \rightarrow \text{products} \quad (2)$$

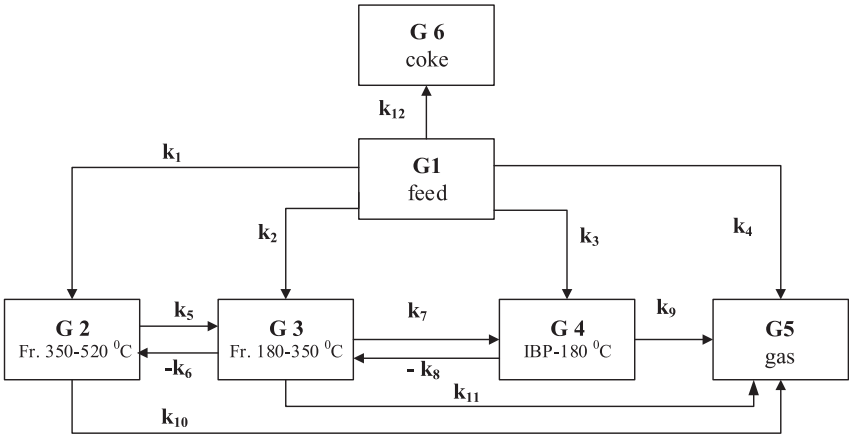

Fig. 1: Kinetic model 2 for HOF hydroconversion.

This model does not include coke as a hydroconversion product (the coke yield is assumed less than 0.5% wt. per feed).

The second model describes the feed conversion to individual components: gas, gasoline, diesel and gas oil fractions, and polycondensation products (coke). The proposed 12-parameter kinetic scheme with partial consideration of secondary reactions is shown in Fig. 1.

It should be noted that secondary reactions can be excluded from consideration by setting the corresponding rate constants to zero (constants k_6 and k_8 in Fig. 1).

The kinetic scheme in Fig. 1 corresponds to a system of linear differential equations describing the rates of first-order reactions:

$$\begin{array}{ll} dG1/d\tau = -R1 - R2 - R3 - R4 - R12 & dG4/d\tau = R3 + R7 - R8 - R9 \\ dG2/d\tau = R1 - R5 + R6 - R10 & dG5/d\tau = R4 + R9 + R10 + R11 \\ dG3/d\tau = R2 + R5 - R6 - R7 + R8 - R11 & dG6/d\tau = R12 \end{array} \quad (3)$$

where: $R1 = k_1*G1$; $R2 = k_2*G1$; $R3 = k_3*G1$; $R4 = k_4*G1$; $R3 = k_3*G1$; $R4 = k_3*G1$; $R5 = k_5*G2$; $R6 = k_6*G3$; $R7 = k_7*G3$; $R8 = k_8*G4$; $R9 = k_9*G4$; $R10 = k_{10}*G2$; $R11 = k_{11}*G3$; $R12 = k_{12}*G1$.

The initial conditions for solving the differential equation systems are:

G1 = a; **G**2 = b; **G**3 = c; **G**4 = d; **G**5 = e; **G**6 = f; where a, b, c, d, e, and f, are the fraction content in the initial feed (%wt.):

$$a + b + c + d + e + f = 100 \quad (4)$$

To solve the differential equation systems, it is assumed that all reactions have pseudo-first order due to excessive hydrogen in the reaction medium. Moreover, a nanosized catalyst is used with a large number of nanosized particles uniformly distributed in the reaction volume. This minimizes diffusion restrictions, since small catalyst particles homogenized in the reaction medium are used.

The differential equation system is solved in two stages:

- solving the reverse problem, which includes finding all the rate constants based on experimental data;
- solving the direct problem, which includes calculating the kinetic parameters using the obtained rate constants.

Experimental part

For the dispersed MoS_2 synthesis, an aqueous precursor (ammonium paramolybdate) solution was emulsified in the feedstock. The formation of a suspension of catalyst particles proceeded with heating the feedstock (in-situ) as a result emulsion dehydration and sulfidation of the catalyst particles with the feed sulfur [8–10]. MoS_2 particles synthesized from the reverse emulsion of an aqueous APM solution have layered contrast with interplanar distance values of 0.62–0.65 nm. Catalyst particles are represented by monoslabs as well as by stackings of 30–500 nm [9]. The experiments were carried out on a pilot upward flow plant with a flow reactor at a pressure of 7 MPa, the volume hydrogen/feedstock ratio of 1000 nl/l, the temperature range of 425–460 °C, and a feed space velocity (V) of 0.7–3.3 h^{-1}.

The feed conversion efficiency was evaluated by the 520 °C+ conversion (Q) and by the amount of coke formed during the hydroconversion and deposited on the reactor walls (G).

$$Q = 100\,(m_0 - m_\tau)/m_0,\ \% \quad (5)$$

where m_0 and m_τ are the masses of vacuum distillation residues (520 °C+) of the initial feedstock and hydrogenate, respectively.

$$G = (M_2 - M_1) \cdot 100/M_C,\ \% \quad (6)$$

where M_1 and M_2 are the reactor masses before and after the experiment; M_C is the feed mass in the experiment.

The conditional contact time (τ) was calculated by the equation:

$$\tau = 60/V, \text{ min} \quad (7)$$

where V is the feed space velocity, h^{-1}.

Results

To determine the formal kinetic parameters, we used the hydroconversion results for several HOF samples, the compositions of which are given in Table 1.

The dependences ln [520 °C+] = f(τ) for all studied feed samples were linear ($R^2 > 0.98$), which indicates the first order of the hydroconversion reaction. Table 2 displays the kinetic characteristics of HOF hydroconversion for model 1 (Equation (2)).

As can be seen from the results obtained, the reaction rate constants at 440 and 450 °C are within 0.0048–0.0295 min^{-1} and 0.0082–0.041 min^{-1}, respectively, and the activation energies are within 137–260 kJ/mol. Fluctuations in the values of the rate constants and activation energies are due to differences in the feedstock properties – viscosity, hydrogen solubility, elemental, and group composition.

The listed parameters can affect the rate and activation energy of hydroconvertion in differently; therefore, it is not always possible to explain fluctuations in the values of k and E_{ak} for different types of feed. For example, the solubility of hydrogen in hydrocarbon media decreases with increasing degree of aromaticity in the series: alkanes, cycloalkanes, arenes. The diffusion rate of hydrogen and feed components, all other things being equal, is determined by the viscosity of the medium, which in turn depends on the content of high molecular weight components - resins and asphaltenes. Natural bitumen (sample 7) is characterized by a high content of asphaltenes, has a highest viscosity, which leads to a high activation energy and relatively low values of the rate constant.

The hydroconversion rate constants of individual SARA components are different and grow in the series: asphaltenes, resins, and hydrocarbons [5]. This is confirmed by comparing the rate constants of the conversion of asphaltenes isolated from feed (sample 5), and the rate constant in the case of feed (sample 5) as a whole (Table 2).

The reaction rate is affected by the presence of distillate hydrocarbon fractions with a boiling point below the experimental temperature in the feed. As a result of the evaporation of distillate fractions, the catalyst

Table 1: Physical and chemical characteristics of heavy oil feedstock.

#	Parameter	Feed sample No.[a]						
		1	2	3	4	5	6	7
1	Density at 20 °C, kg/m^3	941	991	1030	957	1003	1028	1100
2	Cinematic viscosity at 100 °C, mm^2/s	5.25	466	1417	28	394	1796	22 000
3	Coking ability, % wt.	1.5	15.1	17.6	9.01	16.2	16.8	32.3
4	Fractional composition, % wt.							
	IBP, °C	190	376	385	42	354	403	345
	IBP–180 °C	0	0	0	5.5	0	0	0
	180–350 °C	14.8	0	0	17.2	0	0	2.1
	350–520 °C	74.0	15.1	8.9	36.5	16.6	16.3	15.3
	520 °C+	11.2	84.9	91.1	40.8	83.4	83.7	82.5
5	SARA-composition, %wt.							
	Paraffin-naphthene	52.8	14.7	12.0	36.4	14.8	3.3	19.5
	Aromatics	42.0	54.1	53.5	34.3	41.4	53.8	47.9
	Resins	3.6	26.5	22.0	25.1	30.4	33.9	10.2
	Asphaltenes	1.6	4.7	12.5	4.2	13.4	9.0	22.4

[a]Sample 1 – atmospheric residue of gaseous condensate; Samples 2, 3, 5, 6 – vacuum residues from different oils; Sample 4 – heavy bituminous oil; Sample 7 – natural bitumen.

content in the liquid phase of the reactor becomes higher and the partial pressure of hydrogen becomes lower than during the hydroconversion of other feed samples with a reduced content of distillate fractions. This may explain the difference in the reaction rate constants for feed samples 1 and 4 from others.

The experimental results showed that the activation energy of hydroconversion rises with increasing content of asphaltenes in the feed (Fig. 2). This pattern is consistent with previously obtained results of heavy oil hydroconversion in the presence of dispersed MoS_2, according to which, the activation energy increases for the HOF components including: aliphatic hydrocarbons, aromatic hydrocarbons, resins and asphaltenes [5, 6].

According to the experimental results, the Vacuum residue (sample 5) had the dependence of ln k on 1/T (Fig. 3). High values of activation energies and the curve slope in Fig. 3 suggest that the reaction proceeds in the kinetic area.

The obtained values of the kinetic hydroconversion indicators are close to those of the thermal HOF cracking. Thus, during thermal cracking of the vacuum residue of the Arabian oil mixture within 430–445 °C, the reaction rate constant (2) was 0.014–0.028 min^{-1}, and the activation energy was 163–262 kJ/mol [11]. For the thermal cracking of Colombian heavy oil, the activation energy was 220 kJ/mol [12]. The proximity of the kinetic parameters of HOF hydroconversion and thermal cracking can be explained by the low catalyst content in the reaction volume indicating that a major feed amount is converted by the thermal cracking mechanism. A similar conclusion was made in the study of thermal and catalytic hydrocracking of Maya heavy oil in the presence of dispersed MoS_2 [13].

The coke formation is shown schematically in Fig. 4 under the assumption that the sizes of the catalyst nanoparticle associates are larger than the average size of the asphaltene molecules. The primary reactions of the transformation of the structure of asphaltenes are hydrogenolysis of ordinary C–C bonds, which bind the side substituents to the aromatic nucleus of asphaltenes molecules. As a result, due to intermolecular interaction between aromatic layers, ordering occurs with the formation of a supramolecular structure, which is a coke nucleus (Fig. 4b). During hydroconversion in the presence of a catalyst, active hydrogen is generated, which inhibits the process of structuring of aromatic fragments with the formation of coke nuclei.

To clarify the effect of catalyst in the HOF hydroconversion, we should compare the results of experiments on thermal hydroconversion and on catalytic hydroconversion. For this purpose, hydroconversion experiments were conducted with several samples of feed at the same temperatures and different values of the space velocity with the introduction of the catalyst and without catalyst. Based on the change in the amount of the

Table 2: Kinetic parameters of HOF hydroconversion in the presence of in-situ synthesized dispersed nanosize catalyst (MoS_2) (P = 7 MPa).

Feed	T, °C	k, min^{-1}	E_{ac}, kJ/mol
Atmospheric residue, sample 1	445	0.0130	195.3
	450	0.0163	
Heavy oil, sample 4	440	0.0108	201.9
	450	0.0173	
Vacuum residue, sample 2	440	0.0156	175.6
	450	0.0235	
Vacuum residue, sample 5	440	0.0232	223.7
	450	0.0391	
Asphaltenes from vacuum residue (sample 5)	440	0.0048	229.5
	450	0.0082	
Vacuum residue, sample 3	440	0.0128	190.1
	450	0.0200	
Vacuum residue, sample 6	440	0.0156	231.9
	450	0.0268	
Natural bitumen, sample 7[a]	440	0.0078	259.7
	450	0.014	

[a]80% wt. of natural bitumen + 20% wt. of gas-oil.

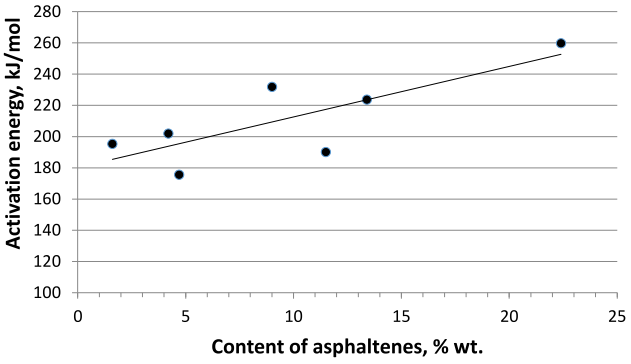

Fig. 2: Dependence of the activation energy on the asphaltenes content in the feedstock during HOF hydroconversion in the presence of in-situ synthesized dispersed nanosize catalyst (MoS_2).

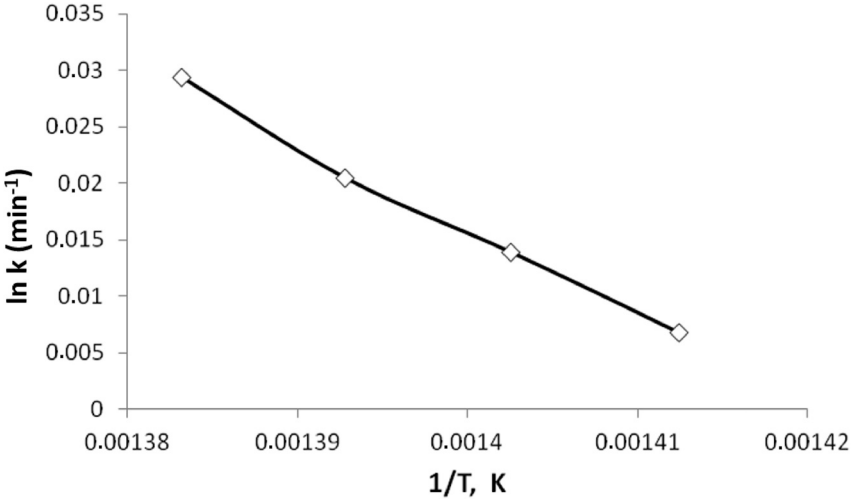

Fig. 3: Dependence of the rate constant logarithm on the hydroconversion temperature. Feedstock: vacuum residue (sample 5). P = 7 MPa, T = 425–450 °C, V = 2.0 h^{-1}. In-situ synthesized dispersed catalyst concentration –0.05% wt. Mo.

520 °C+ fraction in the feed and hydrogenate, taking into account the first order of the reaction, the rate constants *k* were calculated (similar to the calculation of *k* in Table 2). As can be seen from Table 3 the rate of feed conversion into products in thermal hydroconversion experiments (without a catalyst) is significantly higher than in catalytic hydroconversion in the presence of MoS_2. This seems to be associated with that in experiments without a catalyst, one of the main products after HOF conversion is coke (toluene-insoluble polycondensation product). Coke precursors in the thermal HOF processing are asphaltenes that formed radicals under reaction conditions [14]. The presence of polycyclic aromatic fragments in asphaltene molecules (identical to graphite structure) determines easy formation of radical and then polycondensation products during the thermal HOF processing. The coke yield from other SARA components is several times lower than from asphaltenes, and decreases for vacuum residue, aromatic hydrocarbons, saturated hydrocarbons [15]. The polarity of asphaltene molecules determines their high sorption properties with respect to various solid surfaces [16]. The sorption results in much higher asphaltenes concentration in the sorption layer than that in the feedstock. This leads to an increased aggregation and ultimately accelerates coke formation on a solid surface of coke precursors, including the capture of catalyst particles. It was experimentally proven that the addition of small amounts of graphite powder to HOF doubles the coke formation rate [17].

The presence of dispersed MoS_2 significantly decreases the coke yield and increases the distillate fractions yield (Table 3). It was shown in [18] that more than 90% of molybdenum is bound to the feed asphaltenes during the in situ catalyst synthesis. Sorbed asphaltenes are hydrogenated with the formation of lower molecular weight products under hydroconversion conditions (Fig. 5). Direct contact of asphaltenes with catalyst particles contributes to the saturation of radical asphaltene fragments by catalyst-activated hydrogen and reduces coke formation.

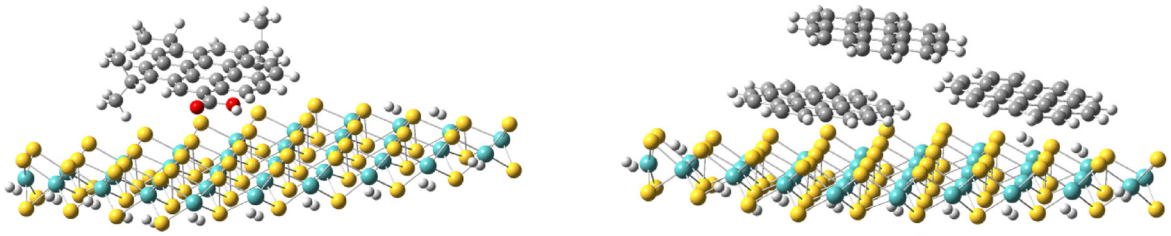

Fig. 4: Scheme of the formation of coke nuclei during the interaction of asphaltene molecules with a MoS_2 catalyst nanoparticle: (a) the stage of formation of the aromatic layer, (b) the formation of a supramolecular structure – coke nuclei due to – the interaction between the layers.

To evaluate the accuracy of the kinetic model (Equation (3)), the hydroconversion results for several HOF samples were used. The rate constants k_i calculated according to the kinetic scheme on Fig. 1; the results are given in Table 4.

Effective feedstock conversion rate constant k_Σ:

$$k_\Sigma = k_1 + k_2 + k_3 + k_4 + k_{12} \tag{8}$$

Activation energy E_{ac} is calculated by the formula:

$$E_{ak} = \frac{RT_1T_2[\ln(k_{\Sigma(1)}) - \ln(\ln(k_{\Sigma(2)}))]}{T_1 - T_2} \tag{9}$$

R = 0.008314 kJ/mol K;

The data analysis in Table 4 shows the following:

- As expected, the effective rate constant k_Σ grows with increasing temperature; the initial feedstock conversion proceeds at a higher rate with increasing temperature;
- Large values of the rate constants for sequential reactions k_1, k_5, and k_7 indicate that the most intense sequential cracking reaction proceeds according to the scheme $G_1 \rightarrow G_2 \rightarrow G_3 \rightarrow G_4$;
- More gaseous products are generated from the G_2 fraction.

Table 3: The effect of in-situ synthesized dispersed catalyst (MoS_2) on HOF hydroconversion results (P = 7.0 MPa, catalyst concentration –0.05% wt. of Mo (per feed)).

Feed sample No.			**3**		**5**		**4**		**1**
Catalyst		–	MoS_2	–	MoS_2	–	MoS_2	–	MoS_2
Temperature, °C			450		440		450		445
Feed space velocity, h^{-1}			2		2		1		1
Yield of products, wt. %									
Gaseous products		3.5	1.97	3.76	2.37	4.35	2.19	3.95	2.38
Hydrogenation fractions	IBP–180 °C	11.9	9.8	14.4	13.9	20.9	19.9	18.4	13.3
	180–350 °C	19.7	19.3	19.3	20.5	40.2	37.4	52.6	56
	350–520 °C	14.7	18.6	20.6	21	20.1	25.8	20.8	23.6
	520 °C+	45.1	50	36.2	41.7	8.42	14.6	3.8	4.7
Toluene insoluble (coke)		5.1	0.33	5.74	0.53	6.03	0.11	0.45	0.02
IBP–520 °C		46.3	47.7	54.3	55.4	81.2	83.1	91.8	92.9
Process parameters									
Conversion of 520 °C+, %		50.5	45.1	56.6	50	79.4	64.2	70.8	63.8
Reaction rate constant, $k \cdot 10^{-2}$, min^{-1}		2.37	2.01	3.5	2.31	2.63	1.71	2.23	1.67

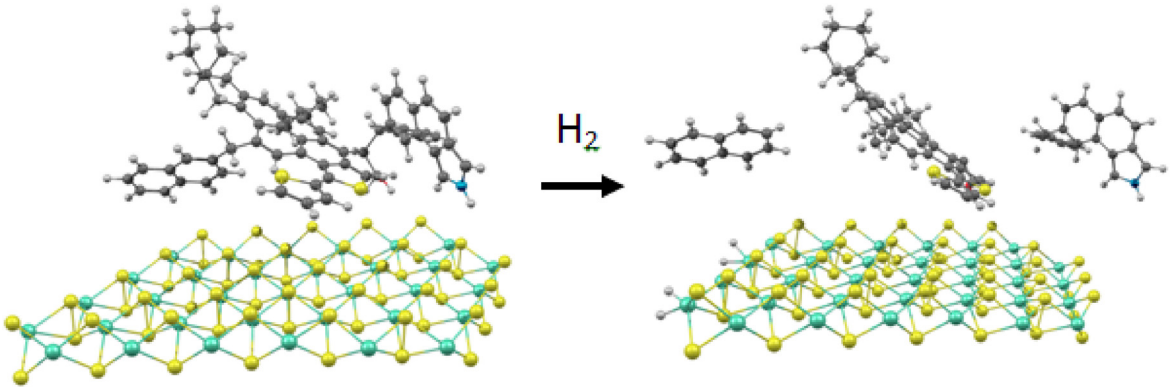

Fig. 5: Hydrocracking scheme for asphaltene molecule in the presence of MoS_2.

Unlike vacuum residues (samples 2 and 5), heavy oil (sample 4) contains a significant amount of distillate fractions with a boiling point of up to 520 °C, the decomposition of which increases the probability of reverse reactions. Apparently, the high content of distillate fractions shifts the equilibrium of chemical reactions towards heavier products. Therefore, the rate constants of the reverse reactions k_6 and k_8 for this sample of feed are significantly higher than for vacuum residues.

Table 5 shows the experimental data on the vacuum residue hydroconversion product yield (sample 5) with the contact time τ at a hydroconversion temperature of 440 °C.

It is worth to be noted that in the process of hydroconversion, coke formation does not begin immediately, but after some time from the start of the reaction. With a short contact time, the coke yield is close to zero, then the coke yield increases exponentially (Table 5). The observed pattern is associated with the behavior of asphaltenes during the thermal processing of HOFs. The hydroconversion process includes the formation of distillate fractions, which leave the reaction zone in a gaseous state, resulting in the decreasing liquid phase volume in the reactor and the growing concentration of asphaltenes [18]. Upon reaching the particular

Table 4: Calculated HOF hydroconversion rate constants: vacuum residue (sample 5 and 2) and heavy oil (sample 4).

Rate constant, min^{-1}	Vacuum residue, sample 5		Vacuum residue, sample 2		Heavy oil, sample 4	
	440	450	440	450	440	450
k_1	0.01482	0.0171	0.01360	0.01960	0.00691	0.01810
k_2	0.00560	0.0126	0.00194	0.00194	0.00210	0.00012
k_3	0.00578	0.0065	0.00110	0.00150	0.00074	0.00001
k_4	0.00007	0.0001	0.00006	0.00006	0.00015	0.00023
k_5	0.01909	0.0184	0.02317	0.02917	0.01800	0.09678
k_6	0.00001	0.0000	0.00012	0.00012	0.00933	0.06135
k_7	0.00690	0.0120	0.01491	0.02151	0.00300	0.02202
k_8	0.00092	0.0054	0.00000	0.00000	0.00002	0.03862
k_9	0.00052	0.0005	0.00002	0.00002	0.00009	0.00011
k_{10}	0.00365	0.0050	0.00088	0.00088	0.00095	0.00013
k_{11}	0.00001	0.0000	0.00046	0.00052	0.00005	0.00020
k_{12}	0.00123	0.0021	0.00095	0.00095	0.00053	0.00134
$k_{\sum}$	0.0275	0.0384	0.01764	0.02404	0.01043	0.01979
E_{ac} kJ/mol		143.1		132.7		274.5

Table 5: Experimental data on the HOF hydroconversion product yield (sample 5). P = 7 MPa, T = 440 °C, catalyst concentration –0.05% wt. of Mo (per feed).

Products	Contact time τ, minute				
	0.0	18.75	24	30	60
G1	83.4	53.8	45.6	42.4	14.6
G2	16.6	24.3	25.4	24.7	21.7
G3	0	13.8	17.2	18.2	32.4
G4	0	7.7	9.3	14.5	19.5
G5	0	0.33	2.45	2.11	4.41
G6	0	0.07	0.05	0.08	7.39

asphaltenes concentration in liquid phase asphaltenes aggregation and mesophase formation, resulting in coke formation are observed [19].

Figure 6 shows the hydroconversion product yields depending on the reaction time calculated by solving the differential equation system based on the obtained rate constants (Table 4). In Fig. 6, the calculated values of hydroconversion product yields over time are compared with the experimental data from Table 5. As follows from Fig. 6, correlation between the calculated data and the experimental data for gas and distillate fractions is satisfactory (R^2 = 0.9903). Consequently, the correct linear model of the first-order HOF hydroconversion reactions has been adopted, and it allows to characterize the component conversion over time and predict the results of the hydroconversion process.

The calculations of the direct kinetic task with the obtained rate constants are shown in the graphic images in Fig. 7, where the lines correspond to the calculated data, and the points correspond to the experimental ones.

The presented data show how the kinetics of the individual component yield over time depends on the HOF chemical nature and its initial fractional composition. Being an important research tool, kinetic modeling allows to extrapolate the product yield for higher reaction time, establish the conversion mechanism for macrocomponents, and determine the optimal yield for the target product.

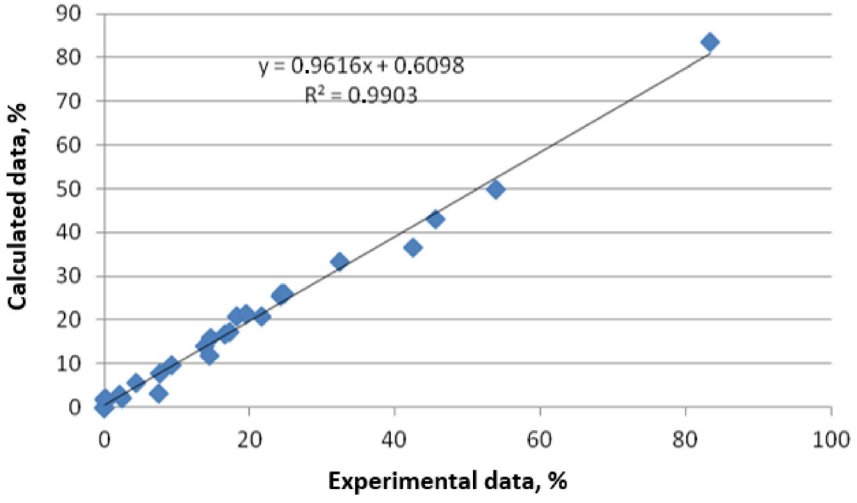

Fig. 6: Comparison of calculated and experimental data on the yield of components (fractions) for vacuum residue hydroconversion (sample 5).

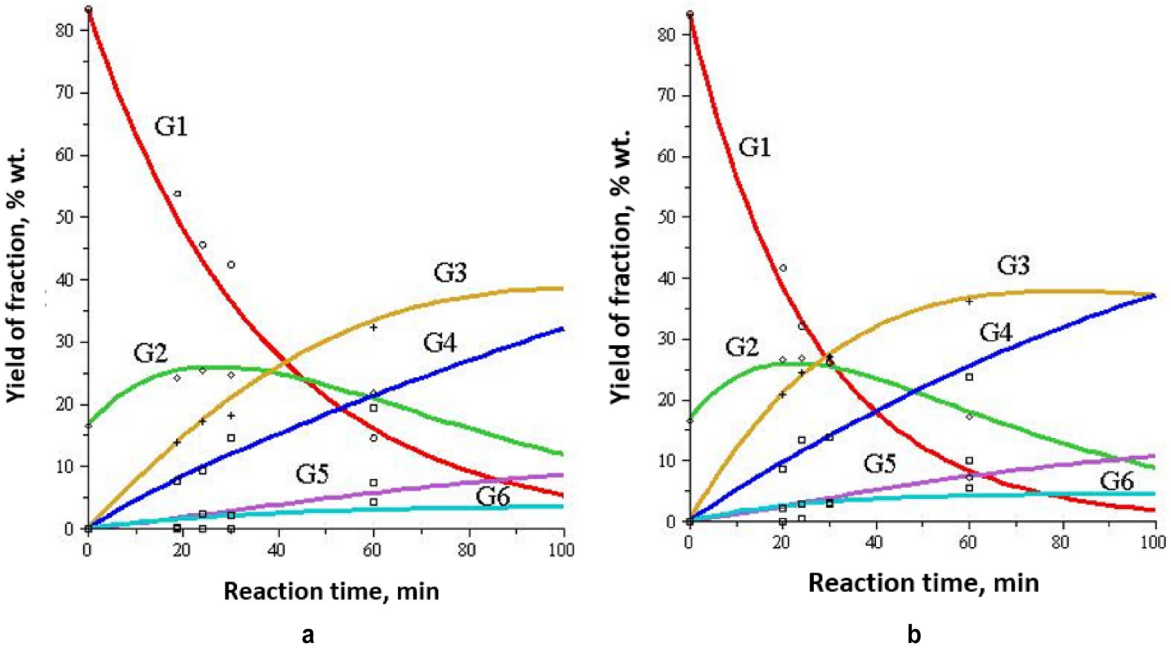

Fig. 7: Dependences of the vacuum residue hydroconversion fractions yield (sample 5) on the reaction time: dots are for experimental data, lines are for calculated data: (a) at T = 440 °C, (b) at T = 450 °C.

Conclusion

A kinetic model of the hydroconversion process has been proposed. The kinetic characteristics of the HOF hydroconversion process in the presence of in-situ synthesized dispersed nanosize catalyst (MoS_2) have been established. During the hydroconversion, transforation of fraction 520 °C+ can proceed in two ways: thermal cracking and hydrocracking. It has been stated that hydroconversion in the presence of in-situ synthesized dispersed nanosize MoS_2 (0.05% wt. Mo per feed) corresponds to a first-order reaction for all studied HOF samples. Large values of the rate constants for sequential reactions k_1, k_5, and k_7 indicate that the most intense cracking reaction proceeds sequentially from heavy fractions to gasoline. It has been shown that the polycondensation product formation results in increasing process rate and decreasing activation energy. It has been proposed that the formed coke serves as the coke formation center and initiates the asphaltenes adsorption followed by thermal polymerization into coke, as displayed by an increase in the rate constant with the growing coke amount in the system.

Funding: This research has been carried out within the TIPS RAS State Program.

References

[1] H. Ahmed, S. Shaban, M. Menoufy, F. El Kady. *Egypt. J. Pet.* **22**, 367 (2013).
[2] M. Rana, J. Ancheyta, S. Sahoo, P. Rayo. *Catal. Today* **220-222**, 97 (2014).
[3] A. Del Bianco, N. Panariti, S. Di Carlo, P. Beltrame, P. Carniti. *Energy Fuel.* **8**, 593 (1994).
[4] N. Panariti, A. Del Bianco, G. Del Piero, M. Marchionna, P. Carniti. *Appl. Catal. A: Gen.* **204**, 215 (2000).
[5] S. Khadzhiev, K. Kadiev, L. Zekel, M. Kadieva. *Pet. Chem.* **58**, 535 (2018).
[6] G. Félix, J. Ancheyta. *Fuel* **241**, 495 (2019).
[7] J. Ancheyta. *Modeling and Simulation of Catalytic Reactors for Petroleum Refining*. John Wiley & Sons, Hoboken, NJ, (2011).
[8] M. Kadieva, S. Khadzhiev, K. Kadiev, T. Yakovenko. *Pet. Chem.* **51**, 426 (2011).

[9] S. Khadzhiev, K. Kadiev, M. Kadieva. *Pet. Chem.* **54**, 323 (2014).
[10] S. Khadzhiev, Kh. Kadiev, M. Kadieva. *Pet. Chem.* **53**, 374 (2013).
[11] A. Sawarkar, A. Pandit, J. Joshi. *Chem. Eng. Res. Des.* **85**, 481 (2007).
[12] L. C. López P´erez. *Kinetic Mechanism for the Cracking of Colombian Heavy Crude Oil Fractions in Refinery Equipments*. M.Sc. in Chemical Engineering. Universidad Nacional de Colombia, Colombia, (2015).
[13] H. Ortiz-Moreno, J. Ramírez, R. Cuevas, G. Marroquín, J. Ancheyta. *Fuel* **100**, 186 (2012).
[14] J. Ancheyta, F. Treiro, M. S. Rana, *Asphaltenes: Chemical Transformation during Hydroprocessing of Heavy Oils*. CRC Press, Boca Raton, London, New York, (2009).
[15] A. Guo, X. Zhang, Z. Wang. *Fuel Process. Technol.* **89**, 643 (2008).
[16] N. Nassar, A. Hassan, P. Pereira-Almao. *Energy Fuel.* **25**, 1017 (2011).
[17] H. Fukuyama, S. Terai, M. Uchida, J. Cano, J. Ancheyta. *Catal. Today* **98**, 207 (2004).
[18] Kh. Kadiev, L. Zekel, M. Kadieva, S. Khadzhiev. *Pet. Chem.* **58**, 519 (2018).
[19] S. Kumar, M. Srivastava. *Carbon Lett.* **16**, 171 (2015).